DETECTING DEFORMATION DUE TO THE 2018 MERAPI VOLCANO ERUPTION USING INTERFEROMETRIC SYNTHETIC APERTURE RADAR (INSAR) FROM SENTINEL-1 TOPS

Suwarsono[1,3,*], Indah Prasasti[1], Jalu Tejo Nugroho[1], Jansen Sitorus[1], Rahmat Arief[2], Khalifah Insan Nur Rahmi[1], Djoko Triyono[3]

[1]Remote Sensing Application Center,

[2]Remote Sensing Technology and Data Center,

Indonesian National Institute of Aeronautics and Space (LAPAN)

[3]Department of Physics, Faculty of Mathematic and Natural Sciences,

Universitas Indonesia

*E-mail: suwarsono@lapan.go.id

Received: 14 June 2019; Revised: 19 August 2019; Approved: 20 August 2019

Abstract. This paper describes the application of Sentinel-1 TOPS (Terrain Observation with Progressive Scans), the latest generation of SAR satellite imagery, to detect displacement of the Merapi volcano due to the May–June 2018 eruption. Deformation was detected by measuring the vertical displacement of the surface topography around the eruption centre. The Interferometric Synthetic Aperture Radar (InSAR) technique was used to measure the vertical displacement. Furthermore, several Landsat-8 Thermal Infra Red Sensor (TIRS) imageries were used to confirm that the displacement was generated by the volcanic eruption. The increasing temperature of the crater was the main parameter derived using the Landsat-8 TIRS, in order to determine the increase in volcanic activity. To understand this phenomenon, we used Landsat-8 TIRS acquisition dates before, during and after the eruption. The results show that the eruption in the May–June 2018 period led to a small negative vertical displacement. This vertical displacement occurred in the peak of volcano range from -0.260 to -0.063 m. The crater, centre of eruption and upper slope of the volcano experienced negative vertical displacement. The results of the analysis from Landsat-8 TIRS in the form of an increase in temperature during the 2018 eruption confirmed that the displacement detected by Sentinel-1 TOPS SAR was due to the impact of volcanic activity. Based on the results of this analysis, it can be seen that the integration of SAR and thermal optical data can be very useful in understanding whether deformation is certain to have been caused by volcanic activity.

Keywords: *Vertical displacement, Landsat-8 TIRS, InSAR, Sentinel-1 TOPS SAR*

1 INTRODUCTION

Ongoing advances in remote sensing Interferometric Synthetic Aperture Radar (InSAR) technology have led to a great expansion in the accessibility of volcano deformation data (Segall, 2013). Optical sensors utilised in the infrared monitoring of volcanic activity have become essential for the monitoring of volcanoes globally (Blackett, 2014). Thermal remote sensing, in particular the Landsat Thematic Mapper (TM), has become reliable as a tool for studying active volcanoes (Wright et al., 2004).

The European Space Agency's (ESA) Sentinel-1A satellite and the United States Geological Survey (USGS), Department of the Interior (DOI) Landsat-8 satellite both acquired SAR and optical data on the Merapi volcano before and during the 2018 eruption. The Sentinel-1 (S-1) mission was based on a constellation of identical C-band

http://dx.doi.org/10.30536/j.ijreses.2019.v16.a3145

(5.547 cm) synthetic aperture radar (SAR) satellites, which now comprise the Sentinel-1 A and Sentinel-B units, to supply data continuity to the ESA's previous European Remote Sensing (ERS) and ENVISAT SAR missions.

The Sentinel-1 A unit was launched in April 2014, reaching its reference orbit on 7 August 2014 (Martinez et al., 2016). A second satellite (Sentinel-1B) was launched in April and made its first observation on 28 April 2016. The Sentinel-1 framework was conceived to supply repeat-pass interferometric capabilities with unprecedented wide area coverage for medium-resolution applications (Torres et al., 2012).

The Sentinel-1A data were collected in the Terrain Observation with Progressive Scans (TOPS) mode, which is similar to a standard Scan-SAR mode, except that the azimuth antenna beam is electronically swept forward in each subswath. The Sentinel-1 is a C-band (5.36 GHz) SAR data product of the ESA. The product has been used in five different modes, namely Stripmap (SM), Interferometric Wide swath (IW), Extra-Wide swath (EW) and Wave (WV). The instrument was designed with one transmitter and two receiver chains. It supports operation in a single and dual polarisation. The data were acquired with a 250 km total swath at 5 m, and a 20 m range and azimuth resolution in a spatial dimension whose incidence angle varies from 29.1° to 46.0° (Periasamy, 2018) (Table 1-1).

The Landsat-8 satellite, the latest generation in the Landsat satellite series from the National Aeronautics and Space Administration (NASA) and USGS, DOI, has advantages over the previous series. Landsat-8 carries an Operational Land Imager (OLI) that comprises nine spectral bands with a spatial resolution of 30 m (15 m for the panchromatic channel) and a Thermal Infrared Sensor (TIRS) capable of measuring surface temperature in two thermal spectral bands with a 100 m spatial resolution (Irons et al., 2012) (Table 1-2).

Table 1-1: Sentinel 1 Interferometric wide Swath Mode SLC Product Parameters (source: Martinez et al., 2016).

Beam	IW1	IW2	IW3
Incidence angles	32.9°	38.3°	43.1°
Slant range resolution	2.7 m	3.1 m	3.5 m
Range Bandwidth	56.5 MHz	48.3 MHz	42.79 MHz
Azimuth resolution	22.5 m	22.7 m	22.6 m
Slant range pixel spacing	2.3 m		
Azimuth pixel spacing	14.1 m		
Ground swath width	250 m		
Orbital repeat cycle	12 days		
Orbit height	698 – 726 km		
Wavelength	5.547 cm		
Polarisation	Single (HH or VV) or Dual (HH+HV or VV+VH)		

Table 1-2: Landsat-8 TIRS spectral bands and spatial resolution (Irons et al., 2012)

Bands	Centre wavelength (μm)	Minimum lower band edge (μm)
10	10.9	10.6
11	12.0	11.5

In this paper, we describe the application of Sentinel-1 TOPS for the purpose of detecting the displacement of the Merapi volcano following the May–June 2018 eruption. Deformation was detected by measuring the vertical displacement of the surface topography around the centre of the eruption.

The novelty of this research is its fusion and integrated use of SAR Sentinel-1 TOPS imagery and Landsat-8 TIRS optical image data to understand with certainty that the deformation resulted from the volcanic eruption activity.

2 MATERIALS AND METHODOLOGY

2.1 Location

The research location is Merapi volcano, located on Java Island. Merapi (110.442° E, 7.542° S) is one of the large

Quaternary central volcanoes of the Sunda arc in Indonesia, which has been shaped by the northward subduction of the Indo-Australian Plate beneath the Eurasian Plate (Hamilton, 1979). Merapi is one of the most active and dangerous volcanoes in the world. It is classified as Type-A Volcano that has erupted several times in history (Kusumadinata, 1979). Merapi alternates between effusive and explosive volcanic activities and self-destruction. The explosivity rate has evolved during the last ten thousand years. Its effusive activities have been characterised by the occurrence of lava flows, the development of a lava dome and the production of a particular 'nuée ardente d'avalanche' known as the Merapi-type nuée ardente.

The explosive stage is frequently accompanied by pyroclastic flows (Sudradjat et al., 2010). Merapi is known for its frequent small to moderate eruptions, pyroclastic flows produced by the collapse of the lava dome, and the large population that has settled on and around the flanks of the volcano that are at risk. The Merapi stratovolcano is located 25–30 km north of the metropolitan region of Yogyakarta, Indonesia (Figure. 2-1), the environs of which are home to more than a million people. It overlies the Java subduction zone and is basically composed of basaltic-andesite tephra, pyroclastic flow, lava and lahar deposits. Eruptions typically occurred every 4 to 6 years during the twentieth century and produced viscous lava domes that collapsed to form pyroclastic flows and subsequent lahars (Surono et al., 2012). According to information from Pusat Vulkanologi dan Mitigasi Bencana Geologi (the Center for Volcanology and Geological Disaster Mitigation), Merapi experienced eruptions during May–June 2019 (Pusat Vulkanologi dan Mitigasi Bencana Geologi, 2019a; 2019b; 2019c; 2019d).

The Merapi stratovolcano complex is covered by the Landsat-8 satellite for path/row 120/065. Administratively, the research sites are included in the areas of the Magelang, Boyolali and Klaten Regency of Central Java Province and Sleman Regency of Yogyakarta, Yogyakarta Special Province. Figure 2-1 shows the location of the research.

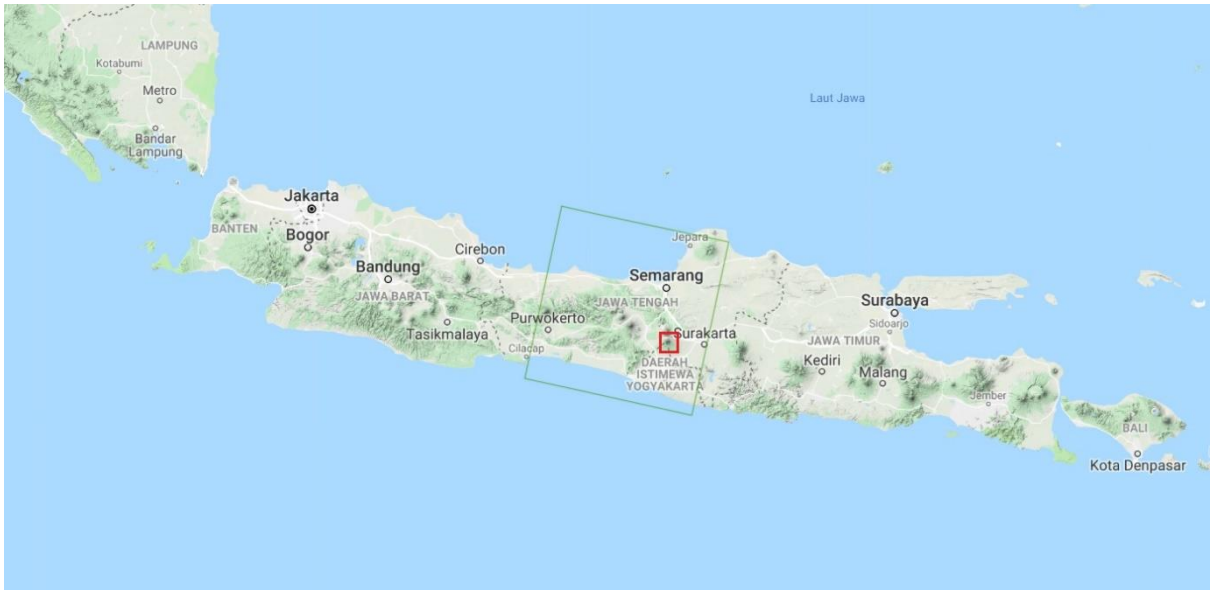

Figure 2-1: Location of the study on Merapi volcano (red rectangle), coverage of Landsat-8 for path/row 120/065 (green rectangle). Map source: http://landsat-catalog.lapan.go.id

2.2 Methods

2.2.1 Interferometric SAR Processing

In order to investigate the displacement over the Merapi volcano due to the May–June 2018 eruption, we generated an interferogram from a pair of Sentinel-1A TOPS images (from ESA) acquired on 28 April and 13 October 2018, spanning the period of the 2018 Merapi eruption, with VV polarisation. The Sentinel-1 IW single-look complex (SLC) datasets were acquired from the Alaska Satellite Facility. This product contained three sub-swaths ('burst SLC'), with mutual overlaps, providing a wide swath at a resolution of 5–20 m (Czikhardt et al., 2017).

We used the IW mode that is capable of providing wide-range swaths as with the ScanSAR technique; however, it almost eliminates the associated problems of scalloping and azimuth variation of the signal-to-noise ratio, noise equivalent sigma zero and azimuth ambiguities (Zan & Guarnieri, 2006). The 1-arcsec resolution NASA Shuttle Radar Topographic Mission (SRTM) Digital Elevation Model (Farr and Kobrick, 2000) was used to remove the topographic phase contribution. We processed InSAR data to estimate the coseismic line-of-sight (LOS) ground displacement.

The interferometric processing methodology of Sentinel-1 TOPS includes selecting a 'burst' that covers the Merapi volcano regions, co-registration, the computation of interferograms, removal of the topographic-related phase with the use of external DEM, adaptive phase filtering (Goldstein & Werner, 1998), phase unwrapping using a minimum cost-flow algorithm (Costantini, 1998), the computation of displacement maps and terrain-corrected geocoding. For the precise co-registration of the Sentinel-1 TOPS, a refinement based on the spectral diversity within bursts and swaths was included (Zan & Guarnieri, 2006). The interferometric image was created by cross-multiplying the master image with the complex conjugate of the slave. The phase represents the phase difference between the two images; the amplitude of both images is multiplied (Veci, 2016).

2.2.2 Landsat-8 TIRS Processing

Several Landsat-8 TIRS imageries were processed to obtain the brightness temperature (BT) of the peak region of Merapi volcano, especially in the crater. We used imagery data from 5 July 2017, 5 May 2018, 25 August 2018 and 12 October 2018. The data were used to provide a description of the temperature, especially in the crater area, before, during and after the eruption. Then, the BT for the band 10 of Landsat-8 TIRS imagery was compiled with SAR. Information about the state of this temperature compiled with displacement from SAR serves as a form of confirmation as to whether the displacement is certain to have originated from volcanic eruption activity or is due to other factors.

The Landsat-8 TIRS Imagery were converted to Top of Atmosphere (TOA) spectral radiance using the following equation (Zanter, 2015):

$$L_\lambda = M_L Qcal + A_L \qquad (2\text{-}1)$$

where L_λ is TOA spectral radiance (Watts/(m^2*srad*μm)), M_L is a Band-specific multiplicative rescaling factor, A_L is a Band-specific additive rescaling factor, and $Qcal$ is the Quantized and calibrated standard product pixel values (DN).

Thereafter, the band 10 of Landsat-8 TIRS imagery was converted to a TOA BT. The band 10 TOA BT was derived using the following equation (Zanter, 2015):

$$T = \frac{K_2}{ln(\frac{K_1}{L_\lambda}+1)} \quad (2\text{-}2)$$

where T is the at-satellite brightness temperature (K), L_λ is TOA spectral radiance, and K_1 and K_2 are Band-specific thermal conversion constants.

3 RESULTS AND DISCUSSION

3.1 Deformation of the Merapi volcano crater due to the 2018 eruption

The eruption in 2018 resulted in relatively small vertical displacement. The phase and coherence derived from the Sentinel-1 TOPS for the Merapi crater during the 2018 eruption can be seen in Figure 3-1. Next, Figure 3-2 shows the the displacement of the peak of the Merapi volcano due to the 2018 eruption.

The crater, centre of eruption and upper slope of the volcano experienced negative vertical displacement. The vertical displacement occurred in the peak area range from -0.260 to -0.063 metres (Figure 3-1 and Figure 3-2). This negative vertical displacement was most likely due to the emptiness of part of the magma chamber just below the crater after the eruption; however, this remains a speculative assertion.

One of the fundamental questions is whether the displacement was the result of magma activity below it or whether it was due to other factors such as tectonic earthquakes or landslides. To explain this, further information is needed in support of the theory that the displacement was the result of magma activity. Therefore, we analysed the temperature changes around the crater. Landsat-8 TIRS imageries were used to analyse the rises in temperature that indicate an increase in volcanic activity.

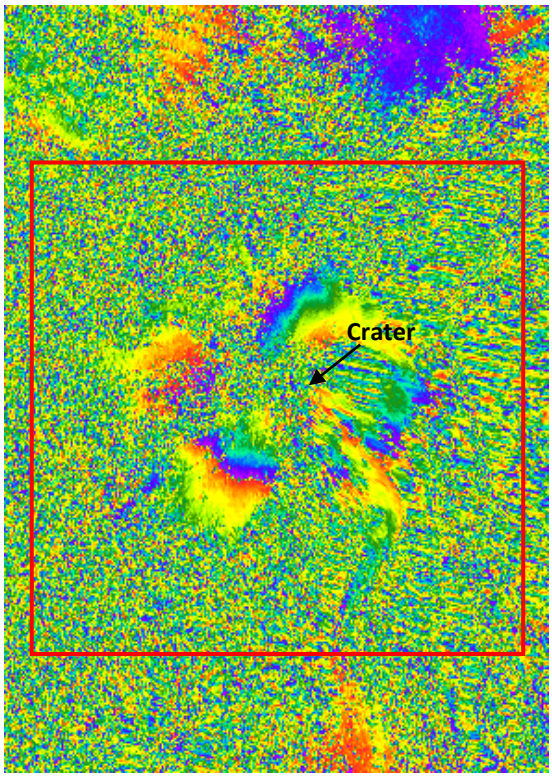

-3.14 3.14

Phase interferogram
28 April – 13 October 2018

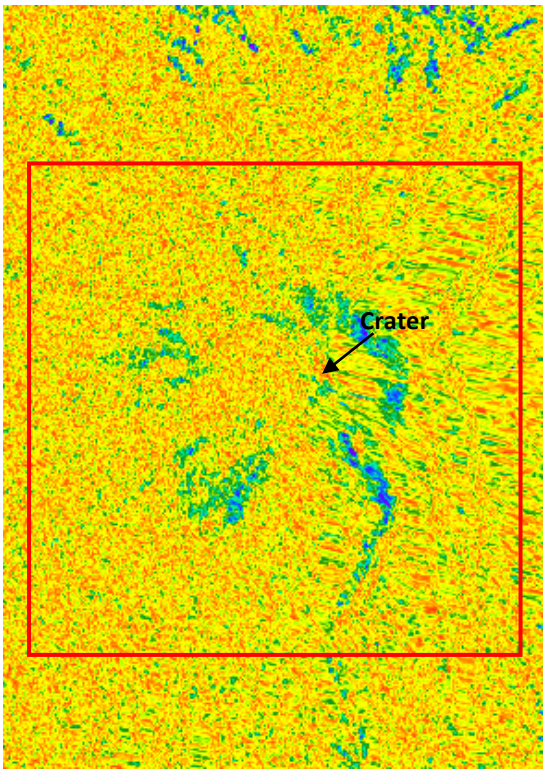

0 1

Coherence
28 April – 13 October 2018

Figure 3-1: The phase interferogram and coherence derived from the Sentinel-1 TOPS of the Merapi stratovolcano during the May–June 2018 eruption.

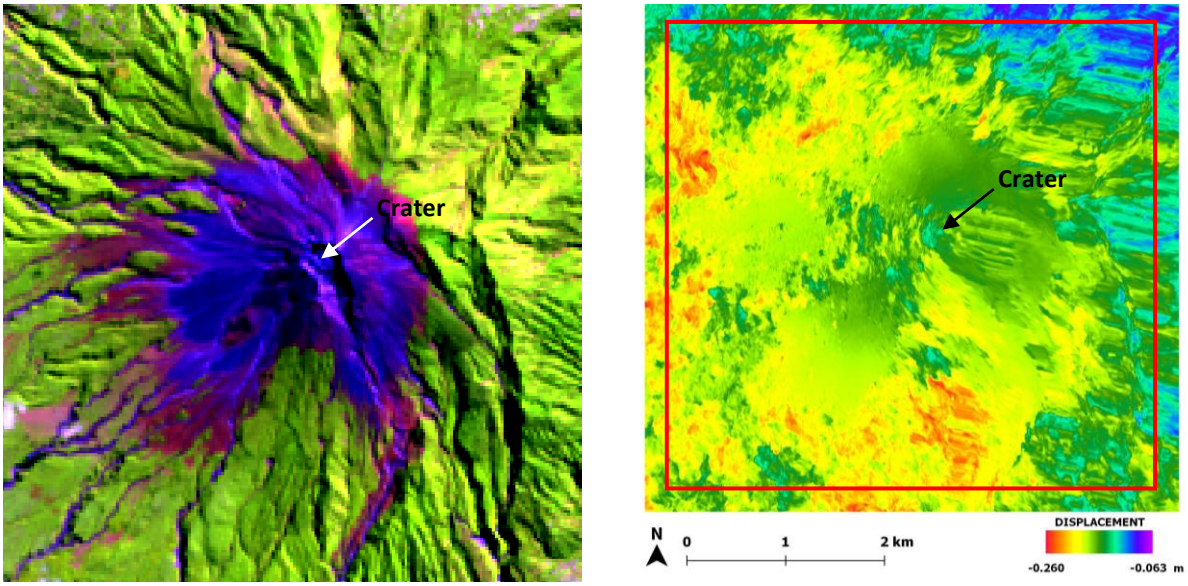

Figure 3-2: Displacement of the peak of the Merapi volcano due to the May–June 2018 eruption (right). The left-hand picture is Landsat-8 RGB 654 dated 5 May 2018. The red rectangle in the right-hand picture shows the boundary when zooming in from Figure 3-1.

3.2 Temperature of the Merapi volcano crater

Based on the Landsat-8 TIRS data, the temperature around the crater was represented among the data by the BT values. The image acquired on 5 July 2017 illustrates the condition prior to the 2018 eruption. The image with an acquisition date of 5 May 2018 shows the condition during the 2018 eruption. Meanwhile, the images acquired on 8 August and 12 October 2018 show the conditions after the 2018 eruption. The results of extracting the BT are shown in Figure (3-3). Based on the Landsat-8 TIRS data, the temperature around the Merapi volcano crater increased during the 2018 eruption. Those areas that experienced an increase in temperature tended to have a pattern and direction associated with the direction of the previous eruption in 2010 (Surono et al., 2012; Yulianto et al., 2012; Pallister et al., 2013; Bignami et al., 2013; Charbonnier et al., 2013), namely in the North East – South East direction. The results of analysis of the temperature increases during the 2018 eruption confirm that the displacement was an impact of the volcanic activity.

4 CONCLUSION

The May–June 2018 Merapi eruption produced a relatively small negative vertical displacement around the crater of the volcano that was detected from Sentinel-1 TOPS SAR. The results of the analysis from Landsat-8 TIRS in the form of an increase in temperature during the 2018 eruption confirm that the displacement was due to the impact of volcanic activity.

Based on the results of this analysis, it can be seen that the integration of SAR and thermal optical data is very useful for understanding with certainty whether deformation has been caused by volcanic activity.

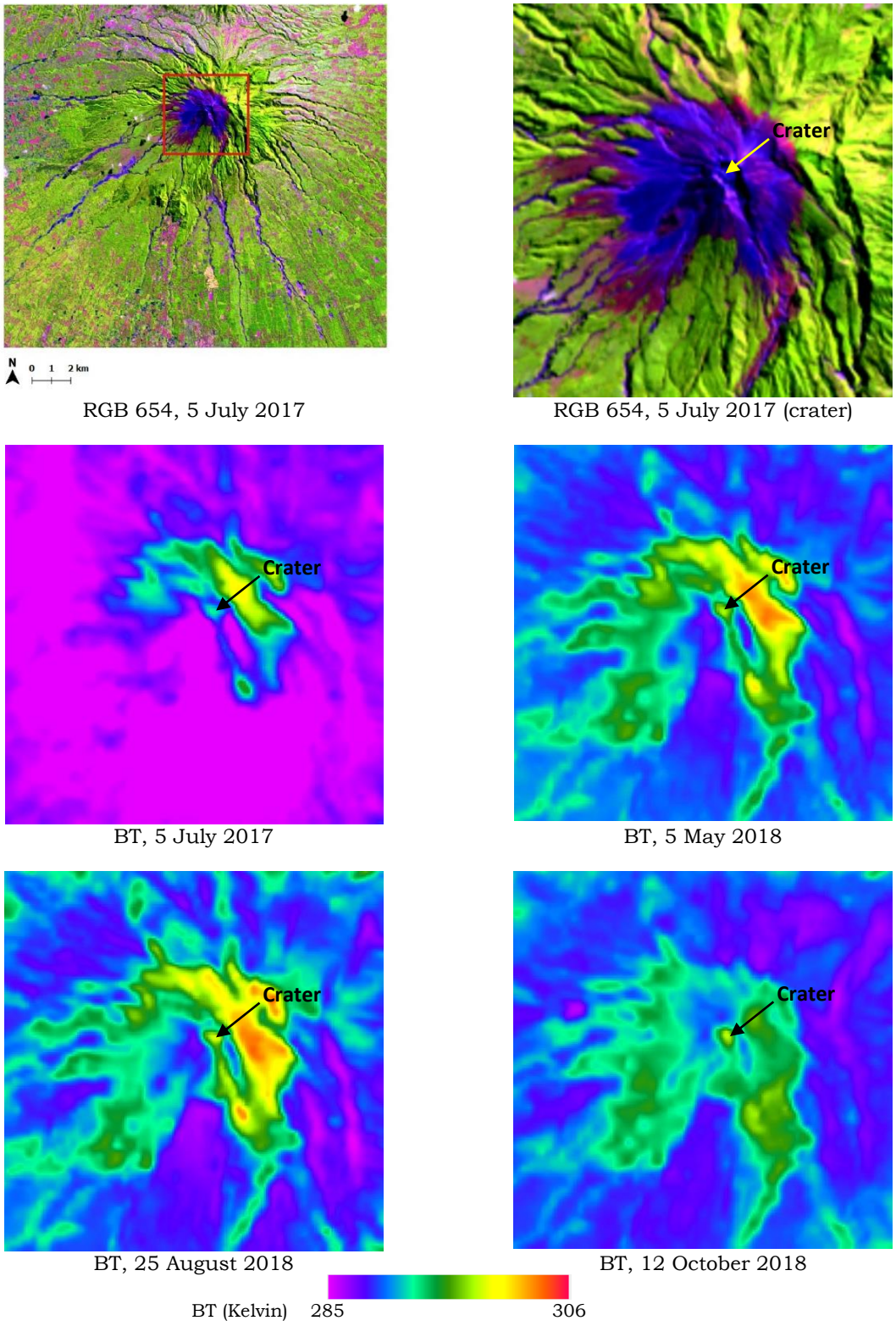

RGB 654, 5 July 2017 | RGB 654, 5 July 2017 (crater)

BT, 5 July 2017 | BT, 5 May 2018

BT, 25 August 2018 | BT, 12 October 2018

Figure 3-3: The spatial pattern of the brightness temperature of the Merapi volcano crater before, during and after the 2018 eruption.

ACKNOWLEDGEMENTS

This paper forms part of research activities entitled 'Development of Optical, SAR, LiDAR and/or GPS Data Fusion'. This research was funded by the Ministry of Research Technology and the Higher Education Republic of Indonesia through the National Innovation System

Research Incentive (INSINAS) programme in 2018 and continues in 2019. Our thanks go to Mr Suhermanto as the Group Leader in this activity. We are also grateful to Dr Mahdi Kartasasmita and Dr Rokhmatuloh who provided suggestions for this research. Thanks also to Dr Hanik Humaida and Mr Gede Suantika from the Center for Volcanology and Geological Disaster Mitigation for the discussion and sharing of information to support this research.

Sentinel-1 TOPS was provided by the Alaska Satellite Facility. Landsat 8 OLI/TIRS was provided by the Remote Sensing Technology and Data Center, LAPAN. The 1-arcsec SRTM DEM was provided by the U.S. Geological Survey (USGS).

REFERENCES

Bignami, C, Ruch, J, Chini, M. et al. (2013). Pyroclastic density current volume estimation after the 2010 Merapi volcano eruption using X-band SAR. *Journal of Volcanology and Geothermal Research, 261,* http://dx.doi.org/10.1016/j.jvolgeores.2013.03.023

Blackett, M. (2014). Early analysis of Landsat-8 thermal infrared sensor imagery of volcanic activity. *Remote Sensing 6,* 2282-2295; doi:10.3390/rs6032282

Charbonnier, S. J, Germa, A., & Connor, C. B. (2013). Evaluation of the impact of the 2010 pyroclastic density currents at Merapi volcano from high-resolution satellite imagery, field investigations and numerical simulations. *Journal of Volcanology and Geothermal Research, 261,* 295–315.

Costantini, M. (1998). A novel phase unwrapping method based on network programming. *IEEE Transactions on Geoscience and Remote Sensing, 36,* 813–821.

Czikhardt, R., Papco, J., Bakon, M. et al. (2017). Ground stability monitoring of undermined and landslide prone areas by means of Sentinel-1 Multi-Temporal InSAR, Case Study from Slovakia. *Geosciences, 7*, 87.

Farr, T. G, & Kobrick, M. (2000). Shuttle radar topography mission produces a wealth of data. *Eos, Transactions American Geophysical, 81*(48), 583–585.

Goldstein, R. M, & Werner, C. L. (1998). Radar interferogram filtering for geophysical applications. *Geophysical Research Letters, 25*(21), 4035–4038.

Hamilton., W (1979). *Tectonics of the Indonesian region.* USGS Professional Paper 1078, 1–345.

Irons, J. R., Dwyer, J. L., & Barsi, J. A. (2012). The next Landsat satellite: The Landsat Data Continuity Mission. *Remote Sensing of Environment, 122*, 11–21.

Kusumadinata (ed) (1979). Data Dasar Gunungapi Indonesia. Direktorat Vulkanologi, Departemen Pertambangan dan Energi Republik Indonesia, Bandung.

Martinez, N. Y., Iraola, P. P., Rodriguez, G. et al. (2016). Interferometric Processing of Sentinel-1 TOPS Data. *IEEE Transactions on Geoscience and Remote Sensing, 54*(4), 2220–2233.

Pallister, J. S., Schneider, D. J., Griswold, J. P. et al. (2013). Merapi 2010 eruption—Chronology and extrusion rates monitored with satellite radar and used in eruption forecasting. *Journal of Volcanology and Geothermal Research, 261,* 144–152.

Periasamy, S. (2018). Significance of dual polarimetric synthetic aperture radar in biomass retrieval: An attempt on Sentinel-1. *Remote Sensing of Environment, 217*, 537–549.

Pusat Vulkanologi dan Mitigasi Bencana Geologi (2019a). Press Release Erupsi Freatik Gunungapi Merapi. Retrieved from: http://www.vsi.esdm.go.id/index.php/gunungapi/aktivitas-gunungapi/2199-press-release-erupsi-freatik-gunungapi-merapi

Pusat Vulkanologi dan Mitigasi Bencana Geologi. (2019b). Laporan Singkat Erupsi Gunung Merapi 11 Mei 2018 pukul 11.00 WIB. Retrieved from: http://www.vsi.esdm.go.id/index.php/gunungapi/aktivitas-gunungapi/2200-laporan-singkat-erupsi-gunung-merapi-11-mei-2018-pukul-1100-wib

Pusat Vulkanologi dan Mitigasi Bencana Geologi (2019c). Informasi Letusan G. Merapi 1 Juni 2018. Retrieved from: http://www.vsi.esdm.go.id/index.php/gunungapi/aktivitas-gunungapi/2242-informasi-letusan-g-merapi-1-juni-2018

Pusat Vulkanologi dan Mitigasi Bencana Geologi (2019d). Siaran Press Letusan G. Merapi 1 Juni 2018. Retrieved from: http://www.vsi.esdm.go.id/index.php/gunungapi/aktivitas-gunungapi/2243-siaran-pers-letusan-g-merapi-1-juni-2018

Segall, P. (2013). *Volcano deformation and eruption forecasting.* Geological Society, London, Special Publications published online March 20, 2013 as doi: 10.1144/SP380.4

Sudradjat, A., Syafri, I., & Paripurno, E. T. (2010). The characteristics of lahar in Merapi Volcano, Central Java as the indicator of the explosivity during Holocene. *Jurnal Geologi Indonesia, 6*(2), 69–74.

Surono, M., Jousset, P., Pallister, J. et al. (2012). The 2010 explosive eruption of Java's Merapi volcano - a '100-year' event. *Journal of Volcanology and Geothermal Research, 241-242*, 121-135.

Torres, R., Snoeij, P., Geudtner, D. et al. (2012). GMES Sentinel-1 mission. *Remote Sensing of Environment, 120*, 9–24.

Veci, L. (2016). Sentinel-1 Toolbox TOPS Interferometry Tutorial. ESA: Paris, France, 1–20.

Wright, R., Flynn, L. P., Garbeil, H. et al. (2004). MODVOLC: near-real-time thermal monitoring of global volcanism. *Journal of Volcanology and Geothermal Research, 135*(1-2), 29–49.

Yulianto, F., Sofan, P., & Khomarudin, M. R. (2012). Extracting the damaging effects of the 2010 of Merapi volcano in Central Java, Indonesia. *Natural Hazards,* doi 10.1007/s11069-012-0438-4

Zan, F. D., & Guarnieri, A. M. (2006). TOPSAR: Terrain observation by progressive scans. *IEEE Transactions on Geoscience and Remote Sensing, 44*(9), 2352–2360.

Zanter, K. (Ed) (2015). *Landsat 8 (L8) Data Users Handbook, Version 1.* Sioux Falls, South Dakota: Department of the Interior, U.S. Geological Survey.